

Dynamics of electron capture into quantum wires

J. F. Ryan, A. C. Maciel, C. Kiener, L. Rota, K. Turner, and J. M. Freyland

Department of Physics, Clarendon Laboratory, Oxford University, Oxford OX1 3PU, United Kingdom

U. Marti, D. Martin, F. Morier-Gemoud, and F. K. Reinhart

Department of Micro- and Optoelectronics, École Polytechnique Fédérale de Lausanne,

Lausanne, CH-1015, Switzerland

(Received 12 October 1995)

We report direct measurements of carrier trapping from three-dimensional states into spatially confined one-dimensional states in GaAs quantum wires. In spite of the small wire volume, very fast trapping (≤ 10 ps) is observed in V-groove wires. Theoretical calculations of trapping via optical-phonon emission, based on an accurate band-structure determination, shows that this arises because of strong overlap of initial extended and final confined electron states.

The dynamics of electron localization is an issue of widespread fundamental interest in condensed matter physics. When localization is induced and controlled by potential structures engineered to atomic monolayer precision using epitaxial growth techniques, the issue acquires great practical significance. For example, spatial confinement of carriers in quantum well lasers significantly enhances efficiency, but trapping into the active region is an important design consideration. In this case optical-phonon emission is predicted to be the dominant trapping mechanism.¹ The process becomes crucial for the operation of quantum wire devices since the very small active volume demands strong coupling to the external region, otherwise trapping is greatly inhibited. In this paper we report, to the best of our knowledge, the first measurements of electron trapping from extended three-dimensional (3D) states into one-dimensional (1D) states of a semiconductor quantum wire structure. Our experimental results, together with a detailed theoretical analysis, show conclusively that quantum effects are important.

We have investigated GaAs quantum wires that are formed by molecular-beam-epitaxial growth in V-shaped channels etched on (001) GaAs substrates. An array of grooves parallel to the $(1\bar{1}0)$ crystallographic axis was produced by holographic photolithography, each 250 nm wide and 110 nm deep. A 5-nm GaAs quantum well was embed-

ded within $(\text{GaAs})_8(\text{AlAs})_4$ superlattice (SL) barriers, growing in a distinctive crescent shape² (see Fig. 1). The layer thickness at the bottom of the groove was measured by transmission electron microscopy (TEM) to be 9.3 nm; it decreases rapidly with distance away from the center of the groove to a value of 2.2 nm, where it merges with the superlattice barriers. The combined effects of layer bending and narrowing give rise to a lateral confining potential, which produces distinct 1D subbands with energy separations of ~ 15 meV.³ As there are no lateral or side-wall quantum wells (cf. Ref. 2), this structure has a relatively simple band structure, which permits the study of trapping directly from 3D extended states into 1D confined states.

Since the localization process depends critically on the shape of the potential and the resulting electron states, we first determined accurate energy levels and wave functions for the structure under investigation. Analytical and numerical approaches, which assume infinite or finite but constant energy potential barriers, have been used previously to provide information on 1D wire states,^{2,4,5} but these methods are not appropriate in the present situation, where we require a detailed knowledge of the barrier states. High-resolution TEM images of the V-groove structure were computer scanned in order to provide a digitized two-dimensional compositional map, and the full 2D cross-sectional potential

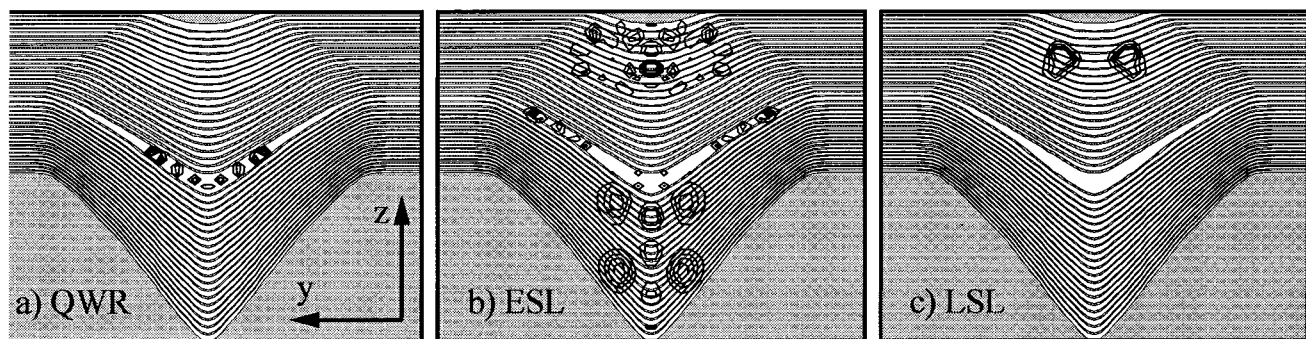


FIG. 1. Potential profile of the GaAs V-groove structure with $(\text{GaAs})_8(\text{AlAs})_4$ SL barriers obtained from TEM data (AlAs layers are shaded), together with contour plots of electronic probability density for (a) the $|1,7\rangle$ QWR state, (b) a typical ESL state, and (c) the lowest-energy LSL state. These states are indicated by arrows in Fig. 2.

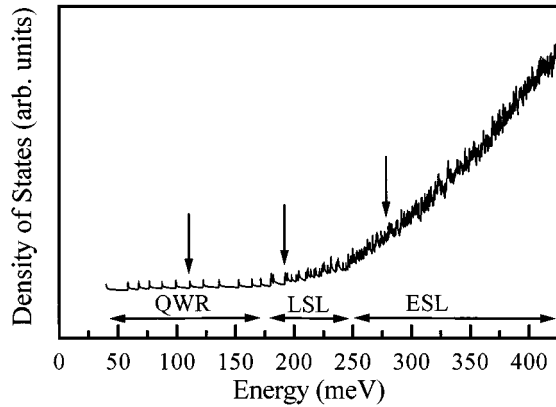


FIG. 2. Calculated electron density of states for the V-groove structure. The arrows indicate the location of the states shown in Fig. 1.

profile was obtained using the accepted 65:35 band offset ratio for GaAs/AlAs heterostructures. The 2D Schrödinger equation was then solved numerically using a plane-wave expansion.⁶ Three distinct types of state are found: (i) 1D confined quantum wire (QWR) states, (ii) bulklike extended superlattice (ESL) states, and (iii) “localized” superlattice (LSL) states.

Figure 1 shows the V-groove structure obtained from the TEM data, together with contour plots of electron probability density for states in each of these categories. z refers to the (001) growth direction, y is the direction of lateral confinement (110), and x is the $(\bar{1}\bar{1}0)$ direction parallel to the wire. The QWR state shown in Fig. 1(a), with quantum numbers $|n_z=1, n_y=7\rangle$, is strongly localized in the wire, which is typical of all states within the $|n_z=1\rangle$ manifold. The ESL states, on the other hand, extend throughout the barrier region [Fig. 1(b)]. Spatial irregularities in the potential profile due to fluctuations in the growth process give rise to the rather complex structure. An important feature of the SL barriers, which is clearly evident in the TEM data, is that the layer thicknesses show systematic spatial variations: the layers below the wire are generally narrower than those above, and furthermore, there is a thickening of the GaAs layers near the center of the groove, whereas the AlAs layers are more closely uniform. This leads to a lower average potential in the central region of the structure, which gives rise to localized states in the barrier which show up quite clearly in the band-structure calculation. These states are localized in the $[1\bar{1}0]$ plane, but are extended in the $(\bar{1}\bar{1}0)$ direction. Figure 1(c) shows the lowest-energy LSL state. The number of such states is dependent on the quality of the sample, and can be reduced by optimizing the growth conditions.

The density of states presented in Fig. 2 shows quite clearly the three spectral regions in question, with the QWR states lying in the low-energy region, and the LSL states lying in the energy range below the ESL continuum. A qualitative indication of the likely strength of the trapping process can be obtained from the spatial overlap of ESL and QWR states. We find that the overlap is relatively large for low-energy ESL states. However, the ESL states also overlap strongly with LSL states, which in turn have practically no overlap with the QWR states. Consequently, electrons that

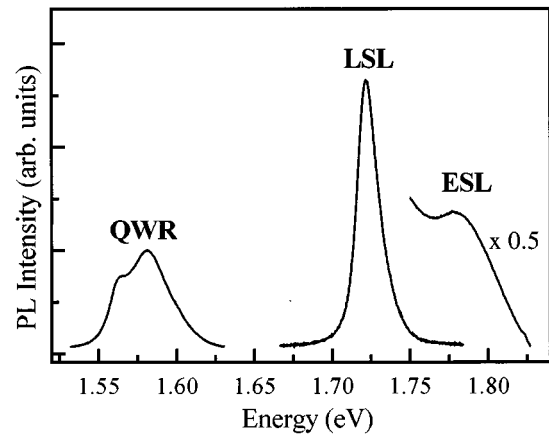


FIG. 3. Time-integrated photoluminescence spectrum of the GaAs V-groove structure at 10 K. The low-energy peaks correspond to QWR recombination. The peak at 1.72 eV is recombination from LSL states, and the weak band at 1.78 eV is ESL luminescence.

are localized into LSL states are unlikely to be trapped into the wires within their recombination time.

Experimental evidence supporting this band-structure analysis, and the implications for carrier trapping, has been obtained using time-resolved photoluminescence (PL) spectroscopy. Dye laser pulses of 5 ps duration were used to photoexcite the V-groove structure, and time-resolved PL spectra were measured using a streak camera with ~ 30 ps resolution. The relative efficiencies of barrier and quantum wire PL, together with direct measurements of rise times and decay times, provide good estimates of the different scattering rates. Figure 3 shows the time-integrated PL spectrum obtained at 10 K with the laser tuned to 1.9 eV, which excites electrons high into the ESL continuum. The laser power was 15 mW, resulting in an estimated density in the quantum wire of $5 \times 10^6 \text{ cm}^{-1}$. The luminescence lines observed at 1.563 eV and 1.580 eV are in excellent agreement with the predicted $|1,1\rangle$ and $|1,2\rangle$ QWR levels, respectively.⁷ The strong line observed at 1.72 eV is in good agreement with our predictions for the lowest-energy LSL state. When the laser power is increased to 90 mW, a weak band appears at 1.78 eV, together with a broad wing that extends to higher energies. This feature has the characteristics of recombination from the ESL states: the signal is weak — approximately 10^{-2} times the combined QWR and LSL signals — due to efficient trapping into these states, and the high-energy wing arises from a nonequilibrium carrier distribution that is unable to cool on the time scale of trapping. Trapping from ESL states into LSL and QWR states is evidently very efficient, and much faster than the carrier recombination time. In the absence of nonradiative effects, the ratio of ESL intensity to the sum of QWR and LSL intensities is equivalent to the ratio of the trapping and recombination times: the latter is expected to be ~ 1 ns, which yields an order of magnitude estimate of 10 ps for the trapping time from ESL states.

Time-resolved PL data are presented in Fig. 4. The $|1,1\rangle$ QWR signal in Fig. 4(a) shows a rise time of ~ 150 ps, and a decay time of ~ 400 ps. The latter is similar to the lifetime measured in quantum wells, and underlines the high quality of the V-groove wires. The rise time is due to relaxation from

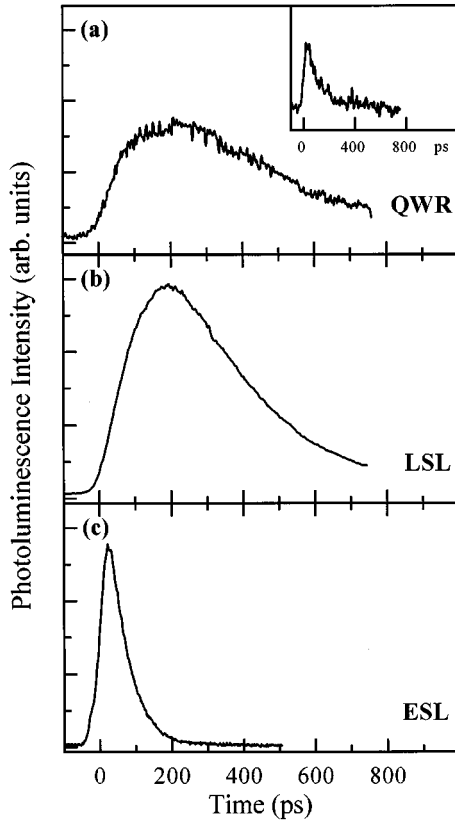


FIG. 4. Time-resolved photoluminescence from (a) the $|1,1\rangle$ QWR state, (b) LSL states, and (c) ESL states.

higher-energy wire states and the barriers. The inset to Fig. 4(a) shows the QWR signal measured at much higher energy where intrawire relaxation effects are less pronounced. The rise time is now within the resolution of the detection system, which directly confirms that trapping into the wires is rapid, occurring within 30 ps.

Figure 4(b) shows the time-resolved LSL luminescence measured under the same experimental conditions as in Fig. 4(a). The rise time is ~ 150 ps, which is similar to the $|1,1\rangle$ QWR behavior, and is characteristic of energy relaxation within the LSL states. The decay time of ~ 400 ps is again typical of radiative recombination; however, it is significantly longer than the rise time of the QWR signal [Fig. 4(a) inset], indicating that trapping from the LSL into the QWR is not a significant effect. In contrast to this behavior, Fig. 4(c) shows that the decay time of the ESL signal is extremely fast, ~ 30 ps, confirming that scattering out of the extended barrier states is very efficient. The fundamental trapping time is likely to be faster than this value, since the experiment was performed at high carrier density ($\sim 10^7$ cm^{-1}) where the effects of carrier-carrier scattering, phonon reabsorption, and final-state filling reduce the trapping rate. The ESL rise time is also extremely fast, which confirms the fact that carrier diffusion is not relevant in this structure (cf. Ref. 8).

Photoluminescence is sensitive to both electron and hole dynamics. Because of their larger effective mass, holes are likely to be trapped more rapidly than electrons, so that the decay of barrier photoluminescence is determined by hole

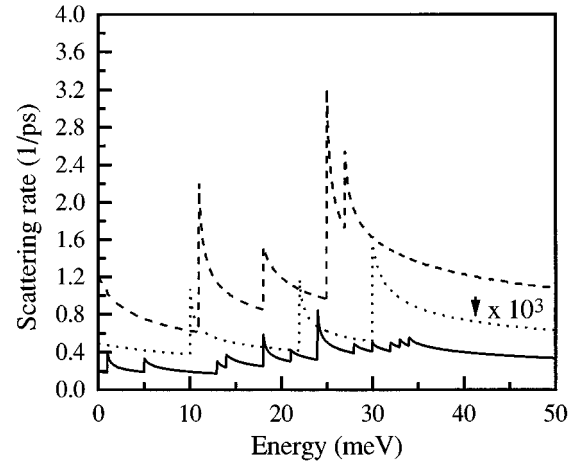


FIG. 5. Calculated trapping rates for electron-LO phonon emission. The solid line represents capture from the ESL state into LSL states, and the dashed line capture into QWR states. The dotted line represents capture from the LSL state at 1.72 eV into QWR states.

trapping, whereas the rise time of wire luminescence is characteristic of electron trapping.⁹ The data presented in Fig. 4 are unable to resolve any difference in these two times, but, nevertheless, they confirm the basic theoretical model described above, and suggest that accurate estimates of the trapping rates can be obtained using the electronic wave functions obtained in the band-structure calculation. We have computed scattering rates for longitudinal optical-phonon emission assuming a bulk phonon approximation. This approach neglects the effects of confined and interface modes, but it is expected, nevertheless, to yield reasonably accurate values for the total scattering rate.¹⁰ Figure 5 shows the rates as a function of initial-state energy. Both $\text{ESL} \rightarrow \text{QWR}$ and $\text{ESL} \rightarrow \text{LSL}$ rates are on the order of 1 ps^{-1} , whereas the $\text{LSL} \rightarrow \text{QWR}$ rate is three orders of magnitude slower. The sharp peaks arise from singularities in the ideal 1D density of states, but in reality they will be smoothed out by inhomogeneous broadening. The calculated trapping rate from ESL states is faster than the experimental time resolution, but it is clearly consistent with the data, and, in particular, with the rate inferred from PL efficiencies. Furthermore, the $\text{LSL} \rightarrow \text{QWR}$ rate is smaller than the measured recombination rate, so that only a small fraction of carriers that get localized in the superlattice barrier are eventually trapped into the wires.

It is important to compare these results with the trapping rates of electrons from bulk states into isolated quantum wells, i.e., $3\text{D} \rightarrow 2\text{D}$ trapping. Electron capture times in the range of 25 ps were obtained in calculations for a separate confinement heterostructure with a 10-nm quantum well within a 100-nm barrier.¹ The relatively long times arise from weak overlap of initial and final states. The use of barriers with an intentionally graded band gap, which increases with distance from the quantum well, dramatically reduces the trapping time to ~ 1 ps, due to the lowest-energy states of the barrier being forced to overlap strongly with the confined states. Our results show that this mechanism is intrinsic to the V-groove quantum wire structure: thickening of both the GaAs quantum wire and SL layers near the center of the V-groove forces the low-energy ESL barrier states to overlap strongly in the lateral direction with the confined

states of the wire. The trapping rate we obtain for the quantum wire, $\sim 1 \text{ ps}^{-1}$, is close to that predicted for optimized graded-barrier quantum well lasers.¹

Our results can be generalized to quantum wires with different barrier compositions and structures. For structures with $(\text{GaAs})_4(\text{AlAs})_2$ SL barriers we find that the above results are only slightly modified. The case of $\text{Al}_x\text{Ga}_{1-x}\text{As}$ alloy barriers is of special interest, since the most successful laser structures fabricated to date use this approach.^{2,11} The self-growth mechanism in the latter case gives rise to a pronounced Ga-rich region in the center of the groove, which leads to the formation of a vertical quantum well,¹² so that lowest-energy barrier states are again constrained close to the

V-groove center, where they have strong overlap with the 1D QWR states. The carrier trapping process in this case involves a sequential $3\text{D} \rightarrow 2\text{D} \rightarrow 1\text{D}$ scattering.

In conclusion, we have reported experimental and theoretical studies of carrier trapping in GaAs V-groove quantum wires. We find that trapping from extended superlattice states into the wires is extremely efficient, and is explained by the special nature of the self-organized growth process, which results in strong overlap of initial and final states.

We wish to acknowledge financial support from EPSRC (UK), and the E.U. through the NANOPT and ULTRAFASST HCM programs, and the Austrian Science Foundation.

¹P.W.M. Blom, C. Smit, J.E.M. Haverkort, and J.H. Wolter, *Phys. Rev. B* **47**, 2027 (1992), and references therein.

²E. Kapon, D.M. Hwang, and R. Bhat, *Phys. Rev. Lett.* **63**, 430 (1989).

³A.C. Maciel, C. Kiener, L. Rota, J.F. Ryan, U. Marti, D. Martin, F. Morier-Gemoud, and F.K. Reinhart, *Appl. Phys. Lett.* **66**, 3039 (1995).

⁴C.J. Anthony and M.J. Kelly, *Semicond. Sci. Technol.* **9**, 36 (1994).

⁵D.S. Citrin and Y-C. Chang, *IEEE J. Quantum Electron.* **29**, 97 (1993).

⁶L. Rota, F. Rossi, P. Lugli, and E. Molinari, in *Proceedings of the International Workshop on Computational Electronics* (Univer-

sity of Leeds, Leeds, UK, 1993), p. 236.

⁷ Transition energies are obtained using calculated electron energies and effective-mass estimates of hole energies (see Ref. 5).

⁸J. Christen, M. Grundman, K. Kapon, E. Colas, D.M. Hwang, and D. Bimberg, *Appl. Phys. Lett.* **61**, 67 (1992).

⁹B. Deveaud, J. Shah, T.C. Damen, and W.T. Tsang, *Appl. Phys. Lett.* **52**, 1886 (1988).

¹⁰L. Rota, F. Rossi, E. Molinari, and P. Lugli, *Phys. Rev. B* **52**, 5183 (1995).

¹¹S. Tiwari, G.D. Petit, K.R. Milkove, F. Legoues, R.J. Davis, and J.M. Woodall, *Appl. Phys. Lett.* **64**, 3536 (1994).

¹²J. Christen, E. Kapon, E. Colas, D.M. Hwang, L.M. Schiavone, M. Grundman, and D. Bimberg, *Surf. Sci.* **267**, 257 (1992).